# Alma Mater Studiorum Università di Bologna
## Archivio istituzionale della ricerca

Immunohistochemical Analysis of Olfactory Sensory Neuron Populations in the Developing Olfactory Organ of the Guppy, Poecilia reticulata (Cyprinodontiformes, Poecilidae)

1

**Immunohistochemical analysis of olfactory sensory neuron populations in the developing**

**olfactory organ of the guppy, *Poecilia reticulata* (Cyprinodontiformes, Poecilidae)**

4

5

Simone Bettini[1]†, Maurizio Lazzari[1]*†, Liliana Milani[1], Maria Gabriella Maurizii[1], Valeria
Franceschini[1]

8

[1] Department of Biological, Geological and Environmental Sciences, University of Bologna,
Via Selmi 3, 40126 Bologna, Italy

11

12

**Olfactory sensory neuron populations in the guppy**

14

16

*   Author for correspondence:

Maurizio Lazzari, Department of Biological, Geological and Environmental Sciences,

University of Bologna, Bologna 40126, Italy

E-mail: maurizio.lazzari@unibo.it

Phone number: +39 051 2094145

22

† The first two authors contributed equally to this work.

24

25    **Abstract**

26    Olfaction is fundamental for sensing environmental chemicals and has obvious adaptive

27    advantages. In fish, the peripheral olfactory organ is composed of lamellae in which the

28    olfactory mucosa contains three main categories of olfactory sensory neurons (OSNs): ciliated

29    (cOSNs), microvillous (mOSNs), and crypt cells. We studied the appearance of these different

30    OSNs during development of *Poecilia reticulata*, given its growing use as animal model

31    system. We performed immunohistochemical detection of molecular markers specific for the

32    different OSNs, carrying out image analyses for marked-cell counting and measuring optical

33    density. *P. reticulata* olfactory organ did not show change in size during the first weeks of life.

34    The proliferative activity increased at the onset of secondary sexual characters, remaining high

35    until sexual maturity. Then it decreased in both sexes, but with a recovery in females, probably

36    in relation to their almost double body growth, compared to males. The density of both cOSNs

37    and mOSNs remained constant throughout development, probably due to conserved functions

38    already active in the fry, independently of the sex. The density of calretinin-positive crypt cells

39    decreased progressively until sexual maturity, whereas the increased density of calretinin-

40    negative crypt cell fraction, prevailing in later developmental stages, indicated their probable

41    involvement in reproductive activities.

42

43    **Keywords:** olfactory epithelium, olfactory sensory neurons, crypt cells, calretinin; G $_{\alpha\ olf}$,

44    PCNA, guppy, immunohistochemistry, image analysis

45

46

**Introduction**

Olfaction is a phylogenetically ancient sense that has a very important role in animal life, being fundamentally related to food research and reproductive behavior (Zeiske et al., 1992). Vertebrates develop an olfactory system that detects odorants and pheromones through their interaction with specialized cell surface receptors on olfactory sensory neurons (OSNs). Olfaction is a form of chemosensation and sensing environmental chemicals has obvious adaptive advantages, thus it is not surprising that a diversity of chemosensory systems has evolved in animals (Poncelet & Shimeld, 2020).

The main types of fish olfactory sensory neurons (OSNs), common to all other vertebrates, are bipolar neurons with dendritic processes that reach the surface of the olfactory epithelium, where they originate olfactory terminal knobs bearing apical differentiations: cilia in ciliated OSNs (cOSNs) and microvilli in microvillous OSNs (mOSNs) (Riddle & Oakley, 1991; Hansen & Zeiske, 1998; Farbman, 2000). Ciliated olfactory sensory neurons (cOSNs) and microvillous olfactory sensory neurons (mOSNs) also differ in location of their cell bodies and length of their dendrites (Morita & Finger, 1998; Hamdani & Døving, 2007). Ciliated OSNs and mOSNs have sensitivities to partially overlapping odorant categories, but project into distinct regions of the olfactory bulb, related to different functions (Hansen et al., 2003; Hamdani & Døving, 2007; Braubach et al., 2012; Bazaes et al., 2013). Other than OSNs, the olfactory epithelium contains other cell types, such as sustentacular cells and basal stem cells.

Fish, in addition to the previously described OSN, also possess a third ovoid-shaped OSN type, the crypt cell (actinopterygian fish, Hansen et al., 1997; Hansen & Finger, 2000; cartilaginous fish, Ferrando et al., 2006, 2007). Crypt cells are located in the upper third of the olfactory epithelium and their apical pole facing the nasal cavity carries both cilia and microvilli. Their axonal projection patterns in the glomerular layer of the olfactory bulb are uneven among

71 species: in *Ictalurus puncatus* and *Carassius Carassius* crypt neuron terminals are localized to

72 the ventral region, suggesting a possible association with pheromone perception and

73 reproductive behavior (Hansen et al. 2003; Weltzien et al., 2003; Hamdani & Døving, 2006).

74 On the other hand, in *Danio rerio*, crypt cells seem to project to one (Ahuja et al., 2013) or two

75 (Braubach et al., 2012; Gayoso et al., 2012) dorsomedial glomeruli supposed to be connected

76 with the medial olfactory tract, that is assumed to convey pheromone detection as well as alarm

77 response (Ahuja et al., 2013). It is also controversial which odorants crypt cells respond to

78 (Hamdani & Døving, 2006; Schmachtenberg, 2006; Hamdani et al., 2008; Vielma et al., 2008),

79 so their function remains unclear. Other two OSN subtypes have been described: kappe cells

80 and pear-shaped neurons (Ahuja et al., 2014; Wakisaka et al., 2017), but they have not currently

81 been described in fish other than zebrafish and it is not sure if they can actually be defined as

82 separate OSN types.

83 The peripheral olfactory organ of fish has a great variability in size, shape and organization in

84 olfactory lamellae (Yamamoto, 1982; Hansen & Zielinski, 2005). With regard to the structure

85 of the peripheral olfactory organ, fish can be distinguished into macrosmatic and microsmatic

86 species (Lazzari et al., 2013). *Poecilia reticulata*, for example, possesses a small olfactory

87 cavity containing a single olfactory lamella, therefore it is considered a typical representative

88 of microsmatic fish (Lazzari et al., 2007).

89 Fish OSNs are directly exposed to environmental water and any substances it contains, toxicants

90 included. Alterations in olfaction can affect fish behavior and survival with possible ecological

91 and socio-economic consequences. *P. reticulata* has become an important model organism for

92 developmental, ecological and toxicological studies (Kinnberg & Toft., 2003; Bettini et al.,

93 2006; Antunes et al., 2017; Souza Trigueiro et al., 2021; Milani et al., 2022), and the acquisition

94 of new information on the development and organization of the olfactory epithelium in this fish

95 will allow us to extend and strengthen its use as model (Bettini et al., 2012, 2016, 2017).

96   Previously in our laboratory, we analyzed in adult *P. reticulata* both the histological and

97   ultrastructural organizations of the peripheral olfactory organ (Lazzari et al., 2007), and the

98   distribution of some molecular markers in the olfactory epithelium (Bettini et al., 2009).

99   Particular attention was paid to crypt cells whose antigenic response in adults distinguished two

100   subpopulations, supporting the possibility that crypt cells are functionally less uniform as

101   supposed (Bettini et al., 2017). Our studies on the development of OSN populations in *P.*

102   *reticulata* have been so far limited to a subpopulation of crypt cells ~~crypt cell subpopulation~~

103   (Bettini et al., 2012). The aim of this work is to study the dynamics of the populations of cOSNs,

104   mOSNs, and a subpopulation of previously unexamined crypt cells, from fish birth to

105   adulthood.

106

**Materials and Methods**

*Animal care and breeding*

Adult (older than 6months) *P. reticulata* (Peters, 1859) of both sexes were purchased locally from Coral Aquarium, Bologna, Italy, acclimated in laboratory conditions using separate aquaria for each sex containing a 1:2 mixture of dechlorinated tap water and distilled water at 27 °C in a 12/12 h light/dark cycle, and fed twice daily with commercial flake food. After 10 days, females were allowed to mate with males, at a ratio of 3:1 to reduce stressful conditions. In the following weeks, aquaria were daily monitored for pregnant females, that were isolated in tanks at the same conditions of aquaria and let give birth. All procedures conformed to the guidelines of European Communities Council Directive (86/609/CEE), the current Italian legislation regarding the use and care of animals, and the guidelines issued by the US National Institutes of Health. The Ethic-Scientific Committee of the University of Bologna also approved this study (protocol no. 17/79/2014).

*Fry collection and tissue sampling*

Newborn individuals were isolated immediately after birth in 5 L tanks and sacrificed at established time points (7, 14, 21, 45 and 90 days safter hatching). We included in the experiment also adult guppies (about 6-month-old). Fish were previously anesthetized with 0.1% 3-aminobenzoic acid ethyl ester (MS-222, Sigma Chemical, St. Louis, MO, USA) and immersion fixed in a modified Bouin's solution (saturated aqueous solution of picric acid and formalin at a ratio of 3:1) for 24 h. Heads from adult guppies were analogously collected and processed, after removal of dorsal cranial vault to facilitate fixation. All samples were washed several times in 0.1 M sodium phosphate buffer, pH 7.4, and decalcified in 10% ethylenediaminetetraacetic acid (EDTA, Fluka, Buchs, SG, CH) in the same buffer for 1-7 days, depending on specimen age and mineralization. Specimens were finally embedded in Paraplast plus (Sherwood Medical, St. Louis, MO, USA; melting point 55–57°C), frontally sectioned (5

132  μm) with Leica 2145 microtome (Leica Microsystems, Milan, IT) and mounted on silanized

133  slides, two sections/slide. Sections of gonads were stained with Hematoxylin and Eosin to

134  determine sex of guppy fry and sexual development.

*Immunohistochemistry*

136  Serial sections were selected for immunohistochemistry. Following stereological methods,

137  every 10th pair of sections a disector was sampled (Bettini et al., 2009, 2012). Slides from 10

138  fish (5 males and 5 females) for each time point were processed. Sections were deparaffinized,

139  rehydrated and immersed in 1% $H_2O_2$ (Sigma Chemical, St Louis, MO, USA) for 20 min at RT

140  to quench endogenous peroxidase. Then antigen retrieval was performed with microwave

141  treatment at 750 W for 10 min in citrate buffer at pH 6.0. Non-specific binding was blocked

142  with 10% normal goat serum (NGS; Vector Laboratories, Burlingame, CA, USA) and 1%

143  bovine serum agglutinin (BSA; Sigma Chemical, St Louis, MO, USA), before incubation in

144  primary antibodies overnight at 4 °C. Then sections were washed and further incubated in

145  horseradish peroxidase (HRP)-conjugated goat anti-rabbit IgG (1:100; Vector Laboratories) for

146  polyclonal primary antibodies and goat anti-mouse IgG (1:100; A4416; Sigma) for monoclonal

147  primary antibody. Finally, the immunoreaction was visualized with 0.1% 3,3-diaminobenzidine

148  substrate (DAB; Sigma Chemical). Sections from zebrafish olfactory organ were chosen for

149  positive controls. Negative controls were obtained by replacing the primary antibody with 10%

150  NGS.

*Antibodies*

152  Primary antibodies used were: 1) polyclonal rabbit anti-calretinin (AB5054 [developed against

153  rat calretinin], Chemicon International, Temecula, CA, USA, 1:1000), a marker for mOSNs

154  (Bettini et al., 2009) and a subpopulation of crypt cells (Bettini et al., 2017); 2) polyclonal rabbit

155  anti-$G_{\alpha\ olf}$ (sc-383; Santa Cruz Biotechnology, Santa Cruz, CA, USA, 1:500), a marker for

156  cOSNs (Gayoso et al., 2011; Braubach et al., 2012; Bettini et al., 2016; Lazzari et al., 2017,

157 2019); 3) monoclonal mouse anti-proliferating cell nuclear antigen (anti-PCNA; Clone PC10;

158 P 8825; Sigma; 1:500) to detect dividing cells (Bettini et al., 2016; Lazzari et al., 2017). All

159 antibodies were already validated in previous literature: anti-calretinin in guppy (Bettini et al.,

160 2017); anti-$G_{\alpha\,olf}$, which recognizes a 42-45 kDa protein under similar experimental conditions,

161 in zebrafish (Gayoso et al., 2011; Braubach et al., 2012), in catfish (Hansen et al., 2003), in

162 lamprey (Frontini et al., 2003), and in goldfish (Hansen et al., 2004).

163 *Image acquisition and statistical analysis*

164 Micrographs were taken using a BEL BlackL 5000 digital camera (BEL Engineering, Monza,

165 Italy) mounted on an Olympus BH-2 microscope (Olympus Italia, Segrate, Italy).

166 Figures were assembled with Adobe Photoshop (CS3; Adobe Systems, San Jose, CA, USA),

167 without content alteration.

168 We used the image analysis software ImageJ (version 1.53t) with Cell Counter plug-in (v.2) to

169 count calretinin-positive crypt cells and PCNA-positive mitotic cells, and calculate epithelial

170 volume and cell density (see Bettini et al., 2012 for more details). Immunostaining patterns of

171 anti-$G_{\alpha\,olf}$ (cOSNs) and anti-calretinin (mOSNs) did not permit cell discrimination and counting

172 (Bettini et al., 2016; Lazzari et al., 2017, 2019, 2021). Therefore, we considered the optical

173 density (OD), since the immunostaining intensity can be regarded as an indirect index of the

174 number of immunopositive cells (Iqbal & Byrd-Jacobs, 2010). In the olfactory epithelium,

175 ImageJ analysis provided average gray values of immunostained regions and background-

176 unstained zones. The OD was then calculated as the logarithm of the ratio between gray values

177 of background and stained Region Of Interest (we excluded the lamina propria and exclusively

178 selected the area of the epithelium, from the apical margin to the basal membrane). Using Excel

179 2019 (Microsoft Corporation, Redmond, WA, USA), data are reported in the histograms as

180 means ± s.e.m. and statistically compared using one-way ANOVA (with LSD (Fisher Least

181    Significant Difference) *post hoc* test) for age groups, and Student's *t*-test for differences

182    between sexes in each group.

183

**Results**

In the first 3 time points considered (from 7 to 21 days of age), guppies were in the fry stage; in the 4th time point, at 45 days after birth, they were in the juvenile stage, when gonads reached their final structure, spermatogenesis started and oogenesis proceeded, secondary sexual characteristics developed and sexual dimorphism began to manifest; in the 5th time point, at 90 days of life fish were in the young stage and they were sexually active, even if sexual maturation was not complete: in females the eggs were not fully matured, while the males, despite having begun to court the females, were not yet capable to produce sperm and fertilize eggs. In the next three months they reached adult stage with fully developed gametes in both sexes (Fig. 1). At this point, fish size growth stopped or slowed down significantly. For more details see Evans et al. (2002) and Koya et al. (2003).

The olfactory organ of *Poecilia reticulata* contains only one olfactory lamella (Fig. 1a) whose surface is covered by the sensory epithelium (Fig. 1b). PCNA immunohistochemistry allowed to evaluate the course of cell proliferation during the considered periods. PCNA-positive cells were usually located in the basal region of the olfactory lamella (Figs. 2a1, 2b1, 2d1, 2a2, 2b2, 2d2). At stages of 7 and 14 days, the immunohistochemical staining was very reduced with very few positive cells detected in the lamellae of both sexes without significant difference between them (Figs. 2a1, 2a2, 2e). From 21 days onwards, the dimensional increase of the olfactory organ was due to a massive and statistically significant cell proliferation compared to the previous stage, but without significant differences between the two sexes (Fig. 2e). At 45 days, mitosis was still intense, comparable to the previous stage (Fig. 2e); the proliferating cells were mainly localized in the posterior edge of the lamella (Figs. 2b1, 2c1, 2b2, 2c2). In males at stage 90, upon reaching the sexual maturity, the proliferation decreased and stabilized showing values comparable to those found in adults. Instead, in females the proliferation continued and appeared to increase again after the mitotic rate decreased at 90 days of age (Fig. 2e). In adults,

209  PCNA-positive cells were still numerous and also present in all the basal layer of female

210  olfactory lamella (Fig. 2d1), while in males they were restricted to some clusters in the posterior

211  region of the lamella (Fig. 2d2). At adult stage, the volume of the olfactory lamella was about

212  twice larger in females compared to males, in line with the ratio of total body size between

213  females and males~~the relative proportions of the whole body of the two sexes~~ (Fig. 2f).

214  Anti-$G_{\alpha\ olf}$ antibody labeled the superficial knobs of ciliated OSNs whose cell bodies were

215  located in the basal third of the olfactory epithelium and showed faint immunopositivity (Fig.

216  3a). The optical density of the immunopositive reaction evolved without significant difference

217  between the two sexes and the various stages considered except for 21 and 45 days, in which

218  the difference between sexes is significant, with the optical density being higher in males at 21

219  days and in females at 45 days (Fig. 3b). At 21 days of life, the optical density of males

220  increased by about 45% compared to the averages measured in previous stages. From 45 days

221  to adulthood the optical density of males returned to the average level recorded in previous fry

222  stages. The optical density of females reached its higher value at 45 days, thus later than in

223  males, then it decreased. However, the statistical analysis did not reveal significant differences

224  between the various stages, even if both F values for females and males were very close to F

225  critical values: female $F_{(P<0.05,5,24)}$=2.465 and male $F_{(P<0.05,5,24)}$=2.610; F critical=2.621.

226  Anti-calretinin immunopositivity was found in mOSNs whose cell bodies were located in the

227  superficial half of the olfactory epithelium (Fig. 3c). The optical density of the

228  immunohistochemical reaction showed no significant difference neither between sexes at any

229  considered stage (Fig. 3d), nor between stages, even if, similarly to what observed for $G_{\alpha\ olf}$

230  immunohistochemistry, both F values for females and males were very close to F critical values:

231  Female $F_{(P<0.05,5,24)}$=2.610 and male $F_{(P<0.05,5,24)}$=2.246; F Critical=2.621. Also in this case, the

232  densities apparently increased in 45-day-old guppies.

233     In addition to mOSNs, anti-calretinin immunohistochemistry also detected a subpopulation of

234     crypt neurons. The intense staining and the shape permitted their easy identification and

235     counting: crypt cells had a typical rounded or ellipsoidal cell body placed close to the free

236     surface of the olfactory epithelium (Figs. 4a, 4b). In the case of crypt cells, the total number of

237     calretinin-positive cells is also ~~directly~~ presented, as their dynamics are exactly opposite to the

238     trend of cell density. When considering the total number of calretinin-positive crypt cells, the

239     value remained low, without significant differences among stages at 7, 14, 21 and 45 days after

240     birth (Fig. 4c). Only in 90 days old fish, crypt cells were significantly more numerous in males

241     than in females. Starting from 45 days onwards, there was a statistically significant increase in

242     the total number of crypt cells compared to previous stages. The total number reached the

243     highest values in adult males and females (Fig. 4c). When the density of immunopositive crypt

244     cells was considered (Fig. 4d), the trend of the values obtained in the various stages appeared

245     reversed compared to the trend of the total number of positive crypt cells. In fact, despite the

246     moderate increase of the total number of calretinin-positive crypt cells, their density decreased

247     up to the minimum value in the adult stage. In females, the density at 7 days after birth was

248     significantly higher than other stages. In the following weeks the values gradually decreased

249     until they stabilized from 45 days onwards. In males, on the other hand, significant differences

250     in the density values of crypt cells among different stages were not observed. Significant

251     differences between the two sexes were present only at 7 days, when the value was higher in

252     females.

253     Comparing the number of calretinin-positive crypt cells obtained in this work with the total

254     number of crypt cells, which are S100-positive, taken from our previous work (Bettini et al.,

255     2009, 2012), we have drawn up Table 1 which shows the percentage ratio between these two

256     types of crypt cells according to age and sex. The subpopulation of calretinin-positive crypt

257     cells remains predominant in both sexes up to 3 weeks, with percentages ranging between 70%

258    and 90% (Table 1); from 45 days onwards, the ratio gradually decreases to 15% in females and

259    30% in males.

260

**Discussion**

The immunohistochemical localization of the selected molecular markers allowed us to follow the dynamics of the different populations of OSNs during the development of the olfactory mucosa of *P. reticulata*. From hatching up to the adult stage, the three main types of OSNs showed different behaviors. In particular, cOSNs and mOSNs showed constant density without particular differences between the stages. Sex-related differences appeared only for cOSNs at 21 and 45 days. Calretinin-positive crypt cells have decreasing density with age. Differences between sexes appeared only at 7 days.

In a previous work (Bettini et al., 2012), we observed that the dimensional increase of the olfactory organ of *P. reticulata* did not follow a linear trend: in the first 3 weeks the lamella did not undergo variations, and only afterwards there was an evident growth, which, after 90 days, led to a clear volumetric difference between males and females. In the present study, the analysis of proliferative activity shows an increase in mitotic cell number in both sexes between 21 and 45 days of life. PCNA-positive cells observed in the early stages of development are exclusively located in the basal layer of the epithelium. Due to their small number, we assume that they predominantly support normal neuronal turnover. The increase in volume does not affect the thickness, but the extent of the lamellar surface: from 21 days onwards, the greatest density of proliferating cells is found in the edges of the olfactory organ, in particular the caudal one, causing a progressive elongation of the lamella. At 90 days of age, the cell division rate stabilizes in males, remaining similar at the male adult stage, on the contrary it further increases in females in the adult stage, as their body growth continues to almost double the size of males. Mousavi-Sabet et al. (2014) reported numerous morphometric changes during the first 50 days of guppy development. While the growth in length of the body was quite progressive, allometric growth pattern of snout length became strongly positive between 15 and 20 days after birth, in line with what we observed in the olfactory organ. We can make some hypotheses in order to explain why the dimensional development of the olfactory organ undergoes this variation at

287   that particular stage. In fish, gonad formation begins 2 weeks before birth and their structure is

288   established at 10-14 days post birth (Koya et al., 2003; Mazzoni et al., 2014). However, sex is

289   unstable in the first weeks after birth and can be affected by administration of androgens, which

290   can lead to sex reversal (Ortega-Salas et al., 2013). The formation of secondary sexual traits

291   (caudal coloration, development of gonopodium in males, etc.), which starts approximately

292   between 2 and 3 weeks of life, appears to be the first indication of guppy sexual identity (Houde,

293   1998; Evans et al., 2002; Koya et al., 2003). In fact, gametogenesis continues during the

294   following weeks and is completed around 90-110 days after birth (Koya et al., 2003), but the

295   formation of rod-shaped gonopodia with clearly visible apical hoods starts courtship activity in

296   males, long before they can produce sperm (Houde, 1998; Evans et al., 2002). Since olfaction

297   is involved in reproduction, the increase in size of the snout (and of the olfactory organ) could

298   be correlated with the morpho-functional differentiation of the sex. But the absence of

299   differences between male and female proliferation patterns could lead to another possible

300   explanation. In accordance with Mousavi-Sabet et al. (2003), the rapid increase in *P. reticulata*

301   snout elongation after 15 days may be related to changing feeding habit, i.e., foraging from

302   water column to water surface.

303   Examining in more detail the development of the olfactory epithelium, we observed that the

304   density of cONSs and mONSs remained constant from the first week of life up to the adult

305   stage, with distinction between the two sexes only for cOSNs at 21 and 45 days. In the

306   comparison between the stages, the apparent increase, however statistically not significant,

307   which is visible for cOSNs between 21 and 45 days, could be a fluctuation simply reflecting

308   the imbalance in the ratio among cell types caused by the intense proliferation activity. It

309   appears evident that cOSNs and mOSNs are associated with the uptake of odorants linked to

310   activities that are functionally independent of sex and stage of development. It is well known

311   that foraging, social interaction, predator and toxicant avoidance and migration are the main

312  behaviors associated with smell in fish (Nikonov & Caprio, 2001; Bazaes et al., 2013; Olivares

313  & Schmachtenberg, 2019).

314  Odorants have been indicatively divided in few molecular classes with different biological

315  functions: amino acids, bile salts, nucleotides, polyamines and pheromones (Nikonov & Caprio,

316  2001; Sato & Sorensen, 2018). Numerous electrophysiological, behavioral and

317  immunohistochemical studies, integrated with analysis of the molecular machinery of OSNs

318  and their projection patterns, made it possible to associate some of those classes of odorants

319  with each of the cell subtypes and suggest their role in the behavioral response (Bazaes et al.,

320  2013; Olivares & Schmachtenberg, 2019). Both cOSNs and mOSNs appear to respond to amino

321  acids in several teleost species (Sato & Suzuki, 2001; Hansen et al., 2003; Schmachtenberg &

322  Bacigalupo, 2004), but cORNs respond preferentially to bile salts, whereas mOSNs are

323  stimulated much more by amino acids and also by nucleotides (Hansen et al., 2003; Sato et al.,

324  2005; Koide et al., 2009; Bazaes et al., 2013; Olivares & Schmachtenberg, 2019). Bile salts,

325  mainly released into the water through feces and urine, are potential social odorants, that could

326  play a role in identification of conspecifics, alarm response and territorial demarcation

327  (Nikonov & Caprio, 2001; Hamdani & Døving, 2007; Bazaes et al., 2013). Nucleotides, instead,

328  serve as feeding cues (Nikonov & Caprio, 2001; Hansen et al., 2003; Wakisaka et al., 2017;

329  Sato & Sorensen, 2018). Amino acids are also a well-known category of food odorants (Hansen

330  et al., 2003; Hara, 2006; Nikonov & Caprio, 2007; Miklavc & Valentinčič, 2012; Sato &

331  Sorensen, 2018), but they appear to be also involved in behaviors other than feeding, such as

332  homing (Yamamoto & Ueda, 2009) and reproduction (Yambe et al., 2006). Taken together

333  these data seem to show that cOSNs are more correlated with social recognition among

334  conspecifics, while mOSNs are more involved in the search for food, even if Biechl et al. (2016)

335  showed that food odors stimulated both OSN subtypes, while only a subpopulation of mOSNs

336  but not cOSNs detected kin odor related signal in zebrafish. These perceptions appear equally

337    important at all stages of development and the constant density of both cell types (cOSNs and

338    mOSNs) that we observed during guppy development seems to be in accordance. However, at

339    the moment the meaning of the difference between sexes at 21 and 45 days for cOSNs remains

340    unclear. This difference could depend on an oscillation, although not significant, of the density

341    values due to the increased proliferation of basal cells that in males is a few days earlier

342    compared to females.

343    Interestingly, it has been observed that in the fish *Astyanax mexicanus*, present in two forms

344    adapted to different environments, the proportions between cOSNs and mOSNs are different

345    (Blin et al., 2018). COSNs were more represented in the surface-dwelling form, which is more

346    oriented towards the sense of sight, while mOSNs were more abundant in the cave-adapted

347    form, in which the sense of smell has predominant importance, given the reduction/absence of

348    eyes. In both morphs, the proliferation, cell death, lifespan and neurogenesis patterns in the

349    developing olfactory epithelium were identical, and very similar also between the two neuron

350    subtypes, analogously to what we observed in guppies. It could have been interesting to

351    compare the number of cOSNs and mOSNs in the guppy, but the immunohistochemical

352    markers, especially the $G_{\alpha\ olf}$, do not allow easy cell counting, so we used an indirect estimate

353    of densities, which thus cannot be compared. A possible solution to be considered to better

354    distinguish and quantify the various OSN populations could be the use of transgenic fish, so far

355    effectively tested by Ma et al. (2018) in zebrafish, but that will be hopefully possible in the

356    future also for *P. reticulata*.

357    The third population of OSNs, crypt cells, has been associated to pheromone perception and

358    reproduction in numerous studies (Hamdani & Døving, 2006; Bazáes & Schmachtenberg, 2012;

359    Ahuja et al., 2013; Bazaes et al., 2013; Olivares & Schmachtenberg, 2019). As further support

360    for this hypothesis, in *Carassius carassius* (Hamdani et al., 2008) the number of crypt cells

361    varies throughout the year, increasing during the summer spawning season. Moreover, the

362    differentiation of crypt cells in the olfactory epithelium of the hermaphrodite *Pseudapocryptes*

363    *lanceolatus* is synchronized with the annual development of ovarian structures in the summer,

364    and they undergo apoptosis when the breeding season is over (Sarkar & De, 2018). We also

365    observed that S100-positive crypt cell development correlates with sex and gonadal maturation

366    in *P. reticulata*, with different dynamics and densities between males and females (Bettini et

367    al., 2012). However, in another study (Bettini et al., 2017), we observed that crypt cells in *P.*

368    *reticulata* do not constitute an immunohistochemically uniform population, identifying a

369    subpopulation of calretinin-positive cells (the population analyzed in the present study). Also,

370    Parisi et al. (2014) described, in zebrafish, a separate population of calretinin-positive crypt

371    cells, even if they showed no co-localization of S100 and calretinin proteins. In the present

372    study, we analyzed how this specific subpopulation of calretinin-positive crypt cells evolves

373    during the first 6 months of postnatal life. Their number increases in line with epithelial size,

374    with no substantial differences between males and females, even if in males it seems to start

375    earlier. The density, however, remains almost constant in males and only slightly decreasing in

376    females, with divergences between the two sexes at 7 days. Particularly interesting is the

377    percentage ratio between this calretinin-positive subpopulation and the totality of crypt cells: at

378    7 days of life, calretinin-positive crypt cells are over 75% in both sexes, but this percentage

379    gradually decreases after 3 weeks, reaching less than 30% in adult males and even 15% in adult

380    females. It can be easily assumed that the two subpopulations have different functions:

381    calretinin-positive cells, similarly to cOSNs and mOSNs, are linked to the perception of odors

382    important from the first day of life to adulthood, while the other crypt cells become numerically

383    preponderant only upon reaching sexual maturity, indicating a role connected to reproduction.

384    Sandulescu et al. (2011) also described an early onset of crypt cell differentiation in zebrafish,

385    at a stage similar to cOSNs and mOSNs, implying a probable functional significance in first

386    life stages. It is known that crypt cells can respond to amino acids (Vielma et al., 2008);

387   moreover, in calcium imaging experiments on the rainbow trout (Bazáes & Schmachtenberg,

388   2012), it was observed that in young fish, crypt cells respond more to amino acids and bile salts,

389   but in mature fish crypt cells are activated preferentially with exposure to gonadal extracts and

390   hormones from the opposite sex. The authors suggested that, during development, the crypt cell

391   population changed sensitivity and function, by replacing common odorant-sensitive cells with

392   pheromone-sensitive ones. Complementing previous research (Bettini et al., 2012, 2017),

393   present study appears to support the simultaneous presence of two distinct subpopulations of

394   crypt neurons, with autonomous functions, modalities and times of development.

395   **Conclusions**

396   In this study we analyzed the development of the olfactory organ of *P. reticulata* that does not

397   show a constant and progressive trend, but has a dimensional increase that begins three weeks

398   after hatching with a massive proliferative activity. The density of cOSNs and mOSNs remains

399   stable, with no differences between stages while sex related distinctions appear only for cOSNs

400   at 21 and 45 days. Calretinin-positive crypt cell density decreases with age despite the

401   simultaneous increase in the total number of these cells, probably due to a large increase in the

402   size of the olfactory epithelium. The results suggest the role of cOSNs, mOSNs and calretinin-

403   positive crypt cells in the uptake of odorants related to basic functions, such as search for food

404   and social relations. However, many gaps remain in the understanding of the sensory

405   capabilities of OSN subtypes, also because other factors influence the olfactory perception,

406   making the data analysis very complex. Many factors appear to influence OSN sensitivity, as

407   documented for example in zebrafish for the integration between alarm-response behavior and

408   mating (Diaz-Verdugo et al., 2019), imprinting among siblings (Biechl et al., 2016), and

409   neuropeptide expression (Kaniganti et al., 2021). Also, environmental changes can alter sensory

410   capacity by modifying the composition of the epithelium, either for pollutants (Iqbal & Byrd-

411   Jacobs, 2010; Dew et al., 2012, 2014, 2016; Lazzari et al., 2017, 2019, 2021) or by improving

412  the olfactory detection capacities, without affecting the organ size, as reported in visual-

413  deprived *Astyanax mexicanus* (Blin et al., 2018).

414  **Financial support**

417

418  **Conflict of interest**

419  The authors declare that they have no conflicts of interest.

420
421

**References**

Ahuja G, Ivandić I, Saltürk M, Oka Y, Nadler W & Korsching SI (2013). Zebrafish crypt neurons project to a single, identified mediodorsal glomerulus. *Sci Rep* **3**, 2063. https://doi.org/10.1038/srep02063

Ahuja G, Nia SB, Zapilko V, Shiriagin V, Kowatschew D, Oka Y & Korsching SI (2014). Kappe neurons, a novel population of olfactory sensory neurons. *Sci Rep* **4**, 4037. https://doi.org/10.1038/srep04037

Antunes AM, Rocha TL, Pires FS, de Freitas MA, Milhomem Cruz Leite VR, Arana S, Moreira PC & Teixeira Saboia-Morais SM (2017). Gender-specific histopathological response in guppies *Poecilia reticulata* exposed to glyphosate or its metabolite aminomethylphosphonic acid. *J Appl Toxicol* **37**(9), 1098-1107. https://doi.org/10.1002/jat.3461

Bazáes A & Schmachtenberg O (2012). Odorant tuning of olfactory crypt cells from juvenile and adult rainbow trout. *J Exp Biol* **215**(10), 1740-1748. https://doi.org/10.1242/jeb.067264

Bazáes A, Olivares J & Schmachtenberg O (2013). Properties, projections, and tuning of teleost olfactory receptor neurons. *J Chem Ecol* **39**(4), 451-464. https://doi.org/10.1007/s10886-013-0268-1

Bettini S, Ciani F & Franceschini V (2006). Cell proliferation and growth-associated protein 43 expression in the olfactory epithelium in *Poecilia reticulata* after copper solution exposure. *Eur J Histochem* **50**(2), 141-146.

Bettini S, Lazzari M, Ciani F & Franceschini V (2009). Immunohistochemical and histochemical characteristics of the olfactory system of the guppy, *Poecilia reticulata* (Teleostei, Poecilidae). *Anat Rec (Hoboken)* **292**(10), 1569-1576. https://doi.org/10.1002/ar.20944

447   Bettini S, Lazzari M & Franceschini V (2012). Quantitative analysis of crypt cell population

448       during postnatal development of the olfactory organ of the guppy, *Poecilia reticulata*

449       (Teleostei, Poecilidae), from birth to sexual maturity. *J Exp Biol* **215**(15), 2711-2715.

450       https://doi.org/10.1242/jeb.069039

451   Bettini S, Lazzari M, Ferrando S, Gallus L & Franceschini V (2016). Histopathological analysis

452       of the olfactory epithelium of zebrafish (*Danio rerio*) exposed to sublethal doses of urea. *J*

453       *Anat* **228**(1), 59-69. https://doi.org/10.1111/joa.12397

454   Bettini S, Milani L, Lazzari M, Maurizii MG & Franceschini V (2017). Crypt cell markers in

455       the olfactory organ of *Poecilia reticulata*: analysis and comparison with the fish model

456       *Danio rerio*. *Brain Struct Funct* **222**(7), 3063-3074. https://doi.org/10.1007/s00429-017-

457       1386-2

458   Biechl D, Tietje K, Gerlach G & Wullimann MF (2016). Crypt cells are involved in kin

459       recognition in larval zebrafish. *Sci Rep* **6,** 24590. https://doi.org/10.1038/srep24590

460   Blin M, Tine E, Meister L, Elipot Y, Bibliowicz J, Espinasa L & Rétaux S (2018).

461       Developmental evolution and developmental plasticity of the olfactory epithelium and

462       olfactory skills in Mexican cavefish. *Dev Biol* **441**(2), 242-251.

463       https://doi.org/10.1016/j.ydbio.2018.04.019

464   Braubach OR, Fine A & Croll RP (2012). Distribution and Functional Organization of

465       Glomeruli in the Olfactory Bulbs of Zebrafish (*Danio rerio*). *J Comp Neurol* **520**(11),

466       2317-2339. https://doi.org/10.1002/cne.23075

467   Dew WA, Wood CM & Pyle GG (2012). Effects of continuous copper exposure and calcium

468       on the olfactory response of fathead minnows. *Environ Sci Technol* **46**(16), 9019-9026.

469       https://doi.org/10.1021/es300670p

470   Dew WA, Azizishirazi A & Pyle GG (2014). Contaminant-specific targeting of olfactory

471   sensory neuron classes: connecting neuron class impairment with behavioural deficits.

472   *Chemosphere* **112**, 519-525. https://doi.org/10.1016/j.chemosphere.2014.02.047

473   Dew WA, Veldhoen N, Carew AC, Helbing CC & Pyle GG (2016). Cadmium-induced

474   olfactory dysfunction in rainbow trout: Effects of binary and quaternary metal mixtures.

475   *Aquat Toxicol* **172**, 86-94. https://doi.org/10.1016/j.aquatox.2015.12.018

476   Diaz-Verdugo C, Sun GJ, Fawcett CH, Zhu P & Fishman MC (2019). Mating suppresses alarm

477   response in zebrafish. *Curr Biol* **29**(15), 2541-2546.e3.

478   https://doi.org/10.1016/j.cub.2019.06.047

479   Evans JP, Pitcher TE & Magurran AE (2002). The ontogeny of courtship, colour and sperm

480   production in male guppies. *J Fish Biol* **60**(2), 495-498. https://doi.org/10.1111/j.1095-

481   8649.2002.tb00299.x

482   Farbman AI (2000). Cell biology of olfactory epithelium. In The neurobiology of taste and

483   smell, Finger TE, Silver WL & Restrepo D (Eds.), pp 131-158. New York: Wiley,

484   Ferrando S, Bottaro M, Gallus L, Girosi L, Vacchi M & Tagliafierro G (2006). Observations of

485   crypt neuron-like cells in the olfactory epithelium of a cartilaginous fish. *Neurosci Lett*

486   **403**(3), 280-282. https://doi.org/10.1016/j.neulet.2006.04.056

487   Ferrando S, Bottaro M, Pedemonte F, De Lorenzo S, Gallus L & Tagliafierro G (2007).

488   Appearance of crypt neurons in the olfactory epithelium of the skate Raja clavata during

489   development. *Anat Rec (Hoboken)* **290**(10), 1268-1272. https://doi.org/10.1002/ar.20584

490   Frontini A, Zaidi AU, Hua H, Wolak TP, Greer CA, Kafitz KW, Li W & Zielinski BS (2003).

491   Glomerular territories in the olfactory bulb from the larval stage of the sea lamprey

492   *Petromyzon marinus*. *J Comp Neurol* **465**(1), 27-37. https://doi.org/10.1002/cne.10811

Gayoso JÁ, Castro A, Anadón R & Manso MJ (2011). Differential bulbar and extra bulbar projections of diverse olfactory receptor neuron populations in the adult zebrafish (*Danio rerio*). *J Comp Neurol* **519**(2), 247-276. https://doi.org/10.1002/cne.22518

Gayoso J, Castro A, Anadón R & Manso MJ (2012). Crypt cells of the zebrafish Danio rerio mainly project to the dorsomedial glomerular field of the olfactory bulb. *Chem Senses* **37**(4), 357-369. https://doi.org/10.1093/chemse/bjr109

Hamdani EH & Døving KB (2006). Specific projection of the sensory crypt cells in the olfactory system in crucian carp, *Carassius carassius*. *Chem Senses* **31**(1), 63-67. https://doi.org/10.1093/chemse/bjj006

Hamdani EH & Døving KB (2007). The functional organization of the fish olfactory system. *Prog Neurobiol* **82**(2), 80-86. https://doi.org/10.1016/j.pneurobio.2007.02.007

Hamdani EH, Lastein S, Gregersen F & Døving KB (2008). Seasonal variations in olfactory sensory neurons—fish sensitivity to sex pheromones explained? *Chem Senses* **33**(2), 119-123. https://doi.org/10.1093/chemse/bjm072

Hansen A & Finger TE (2000). Phyletic distribution of crypt-type olfactory receptor neurons in fishes. *Brain Behav Evol* **55**(2), 100-110. https://doi.org/10.1159/000006645

Hansen A & Zeiske E (1998). The peripheral olfactory organ of the zebrafish, *Danio rerio*: an ultrastructural study. *Chem Senses* **23**(1), 39-48. https://doi.org/39-48. 10.1093/chemse/23.1.39

Hansen A & Zielinski BS (2005). Diversity in the olfactory epithelium of bony fishes: development, lamellar arrangement, sensory neuron cell types, and transduction components. *J Neurocytol* **34**(3-5), 183-208. https://doi.org/10.1007/s11068-005-8353-1

Hansen A, Eller P, Finger TE & Zeiske E (1997). The crypt cell: a microvillous ciliated olfactory receptor cell in teleost fishes. Nineteenth annual meeting of the association for chemoreception sciences (AchemS XIX) and the twelfth international symposium on

518     olfaction    and    taste    (ISOT    XII)    *Chem*    *Senses*    **22**(6),    694-695.

519       https://doi.org/10.1093/chemse/22.6.635

520 Hansen A, Rolen SH, Anderson K, Morita Y, Caprio J & Finger TE (2003). Correlation between

521       olfactory receptor cell type and function in the channel catfish. *J Neurosci* **23**(28), 9328 -

522       9339. https://doi.org/10.1523/JNEUROSCI.23-28-09328.2003

523 Hansen A, Anderson KT & Finger TE (2004). Differential distribution of olfactory receptor

524       neurons in goldfish: structural and molecular correlates. *J Comp Neurol* **477**(4), 347-359.

525       https://doi.org/10.1002/cne.20202

526 Hara TJ (2006). Feeding behaviour in some teleosts is triggered by single amino acids primarily

527

      through    olfaction.    *J*    *Fish*    *Biol*    **68**(3),    810-825.    https://doi.org/10.1111/j.0022-

528       1112.2006.00967.x

529 Houde AE (1998). 2. Reproductive biology and sexual behavior. In *Sex, color, and mate choice*

530       *in guppies*, Houde AE (Ed.), pp. 29-44. Princeton: Princeton University Press.

531       https://doi.org/10.1515/9780691207261-003

532   Iqbal T & Byrd-Jacobs C (2010). Rapid degeneration and regeneration of the zebrafish

533       olfactory epithelium after triton X-100 application. *Chem Senses* **35**(5), 351-361.

534       https://doi.org/10.1093/chemse/bjq019

535 Kaniganti T, Deogade A, Maduskar A, Mukherjee A, Guru A, Subhedar N & Ghose A

536       (2021). Sensitivity of olfactory sensory neurons to food cues is tuned to nutritional states

537       by Neuropeptide Y signaling. *J Neurochem* **159**(6), 1028-1044.

538       https://doi.org/10.1111/jnc.15488

539 Kinnberg K & Toft G (2003). Effects of estrogenic and antiandrogenic compounds on the testis

540       structure of the adult guppy (*Poecilia reticulata*). *Ecotoxicol Environ Saf* **54**(1), 16-24.

541       https://doi.org/10.1016/s0147-6513(02)00010-6

542 Koide T, Miyasaka N, Morimoto K, Asakawa K, Urasaki A, Kawakami K & Yoshihara Y

543 (2009). Olfactory neural circuitry for attraction to amino acids revealed by transposon

544 mediated gene trap approach in zebrafish. *Proc Natl Acad Sci USA* **106**(24), 9884-9889.

545 https://doi.org/10.1073/pnas.0900470106

546 Koya Y, Fujita A, Niki F, Ishihara E & Miyama H (2003). Sex differentiation and pubertal

547 development of gonads in the viviparous mosquitofish, *Gambusia affinis*. *Zoolog Sci*

548 **20**(10), 1231-1242. https://doi.org/10.2108/zsj.20.1231

549 Lazzari M, Bettini S, Ciani F & Franceschini V (2007). Light and transmission electron

550 microscopy study of the peripheral olfactory organ of the guppy, *Poecilia reticulata*

551 (Teleostei, Poecilidae). *Microsc Res Tech* **70**(9), 782-789.

552 https://doi.org/10.1002/jemt.20487

553 Lazzari M, Bettini S & Franceschini V (2013). Immunocytochemical characterization of

554 olfactory ensheathing cells in fish. *Brain Struct Funct* **218**(2), 539-549.

555 https://doi.org/10.1007/s00429-012-0414-5

556 Lazzari M, Bettini S, Milani L, Maurizii MG & Franceschini V (2017). Differential response

557 of olfactory sensory neuron populations to copper ion exposure in zebrafish. *Aquatic*

558 *Toxicol* **183**, 54-62. https://doi.org/10.1016/j.aquatox.2016.12.012

559 Lazzari M, Bettini S, Milani L, Maurizii MG & Franceschini V (2019). Differential nickel-

560 induced responses of olfactory sensory neuron populations in zebrafish. *Aquatic Toxicol*

561 **206**, 14-23. https://doi.org/10.1016/j.aquatox.2018.10.011

562 Lazzari M, Bettini S, Milani L, Maurizii MG & Franceschini V (2021). Response of olfactory

563 sensory neurons to mercury ions in zebrafish: an immunohistochemical study. *Microsc*

564 *Microanal* **28**(1), 227-242. https://doi.org/10.1017/S1431927621013763

565 Ma EY, Heffern K, Cheresh J & Gallagher EP (2018). Differential copper-induced death and

566 regeneration of olfactory sensory neuron populations and neurobehavioral function in

larval zebrafish. *Neurotoxicology* **69,** 141-151. https://doi.org/10.1016/j.neuro.2018.10.002

Mazzoni TS, Grier HJ & Quagio-Grassiotto I (2014). Male gonadal differentiation and the paedomorphic evolution of the testis in teleostei. *Anat Rec* **297**(6), 1137-1162. https://doi.org/10.1002/ar.22915

Miklavc P & Valentinčić T (2012). Chemotopy of amino acids on the olfactory bulb predicts olfactory discrimination capabilities of zebrafish *Danio rerio*. *Chem Senses* **37**(1), 65-75. https://doi.org/10.1093/chemse/bjr066

Milani L, Cinelli F, Iannello M, Lazzari M, Franceschini V & Maurizii MG (2022). Immunolocalization of Vasa, PIWI, and TDRKH proteins in male germ cells during spermatogenesis of the teleost fish *Poecilia reticulata*. *Acta Histochem* **124**(3), 151870. https://doi.org/10.1016/j.acthis.2022.151870

Morita Y & Finger TE (1998). Differential projections of ciliated and microvillous olfactory receptor cells in the catfish, *Ictalurus punctatus*. *J Comp Neurol* **398**(4), 539-550. https://doi.org/10.1002/(sici)1096-9861(19980907)398:4<539::aid-cne6>3.0.co;2-3

Mousavi-Sabet H, Azimi H, Eagderi S, Bozorgi S & Mahallatipour B (2014). Growth and morphological development of guppy *Poecilia reticulata* (Cyprinodontiformes, Poeciliidae) larvae. *Poec Res* **4**(1), 24-30. http://www.pr.bioflux.com.ro/docs/2014.24-30.pdf

Nikonov AA & Caprio J (2001). Electrophysiological evidence for a chemotopy of biologically relevant odors in the olfactory bulb of the channel catfish. *J Neurophysiol* **86**(4), 1869-1876. https://doi.org/10.1152/jn.2001.86.4.1869

Nikonov AA & Caprio J (2007). Highly specific olfactory receptor neurons for types of amino acids in the channel catfish. *J Neurophysiol* **98**(4), 1909-1918. https://doi.org/10.1152/jn.00548.2007

592    Olivares J & Schmachtenberg O (2019). An update on anatomy and function of the teleost

593    olfactory system. *PeerJ* **7**, e7808. https://doi.org/10.7717/peerj.7808

594    Ortega-Salas A, Reyes-Bustamante H & Reyes BH (2013). Sex reversal, growth, and survival

595    in the guppy *Poecilia reticulata* (Cyprinodontiformes: Poeciliidae) under laboratory

596    conditions. *UNED Res J* **5**(2), 245-248. https://doi.org/10.22458/urj.v5i2.278

597    Parisi V, Guerrera MC, Abbate F, Garcia-Suarez O, Viña E, Vega JA & Germanà A (2014).

598    Immunohistochemical characterization of the crypt neurons in the olfactory epithelium of

599    adult zebrafish. *Ann Anat* **196**, 178-182. https://doi.org/10.1016/j.aanat.2014.01.004

600    Poncelet G & Shimeld SM (2020). The evolutionary origins of the vertebrate olfactory system.

601    *Open Biol* **10**(12), 200330. https://doi.org/10.1098/rsob.200330

602    Riddle DR & Oakley B (1991). Evaluation of projection patterns in the primary olfactory

603    system    of    rainbow    trout.    *J    Neurosci*    **11**(12),    3752-3762.

604    https://doi.org/10.1523/JNEUROSCI.11-12-03752.1991

605    Sandulescu CM, Teow RY, Hale ME & Zhang C (2011). Onset and dynamic expression of

606    S100 proteins in the olfactory organ and the lateral line system in zebrafish development.

607    *Brain Res* **1383**, 120-127. https://doi.org/10.1016/j.brainres.2011.01.087

608    Sarkar SK & De SK (2018). Ultrastructure based morphofunctional variation of olfactory crypt

609    neuron    in    a    monomorphic    protogynous    hermaphrodite    mudskipper    (Gobiidae:

610    Oxudercinae) (*Pseudapocryptes lanceolatus* [Bloch and Schneider]). *J Microsc Ultrastruct*

611    **6**(2), 99-104. https://doi.org/10.4103/JMAU.JMAU_18_18

612    Sato K & Sorensen PW (2018). The chemical sensitivity and electrical activity of individual

613    olfactory sensory neurons to a range of sex pheromones and food odors in the goldfish.

614    *Chem Senses* **43**(4), 249-260. https://doi.org/10.1093/chemse/bjy016

615    Sato K & Suzuki N (2001). Whole-cell response characteristics of ciliated and microvillous

616        olfactory receptor neurons to amino acids, pheromone candidates and urine in rainbow

617        trout. *Chem Senses* **26**(9), 1145-1156. https://doi.org/10.1093/chemse/26.9.1145

618    Sato Y, Miyasaka N & Yoshihara Y (2005). Mutually exclusive glomerular innervation by two

619        distinct transgenic zebrafish. *J Neurosci* **25**(20), 4889-4897.

620        https://doi.org/10.1523/JNEUROSCI.0679-05.2005

621    Schmachtenberg O (2006). Histological and electrophysiological properties of crypt cells from

622        the olfactory epithelium of the marine teleost *Trachurus symmetricus. J Comp Neurol*

623        **495**(1), 113-121. https://doi.org/10.1002/cne.20847

624    Schmachtenberg O & Bacigalupo J (2004). Olfactory transduction in ciliated receptor neurons

625        of the Cabinza grunt, *Isacia conceptionis* (Teleostei: Haemulidae). *Eur J Neurosci* **20**(12),

626        3378-3386. https://doi.org/10.1111/j.1460-9568.2004.03825.x

627    Souza Trigueiro NS, Gonçalves BB, Cirqueira Diaz F, Celmade Oliveira Lima E, Lopes Rocha

628        T & Teixeira Saboia-Morais SM (2021). Co-exposure of iron oxide nanoparticles and

629        glyphosate-based herbicide induces DNA damage and mutagenic effects in the guppy

630        (*Poecilia reticulata*). *Environ Toxicol Pharmacol* **81**, 103521.

631        https://doi.org/10.1016/j.etap.2020.103521

632    Vielma A, Ardiles A, Delgado L & Schmachtenberg O (2008). The elusive crypt olfactory

633        receptor neuron: evidence for its stimulation by amino acids and cAMP pathway agonists.

634        *J Exp Neurol* **211**(15), 2417-2422. https://doi.org/10.1242/jeb.018796

635    Wakisaka N, Miyasaka N, Koide T, Masuda M, Hiraki-Kajiyama T & Yoshihara Y (2017). An

636        adenosine receptor for olfaction in fish. *Curr Biol* **27**(10), 1437-1447.

637        https://doi.org/10.1016/j.cub.2017.04.014

638 Weltzien FA, Hoglund E, Hamdaniel H & Døving KB (2003). Does the lateral bundle of the

639 medial olfactory tract mediate reproductive behavior in male crucian carp? *Chem Senses*

640 **28**(4), 293-300. https://doi.org/10.1093/chemse/28.4.293

641 Yamamoto M (1982). Comparative morphology of the peripheral olfactory organ in teleosts. In

642 *Chemoreception in fishes*, Hara TJ (Ed.), pp. 39–59. Amsterdam: Elsevier.

643 Yamamoto Y & Ueda H (2009). Behavioral responses by migratory chum salmon to amino

644 acids in natal stream water. *Zoolog Sci* **26**(11), 778-782. https://doi.org/10.2108/zsj.26.778

645 Yambe H, Kitamura S, Kamio M, Yamada M, Matsunaga S, Fusetani N & Yamazaki F (2006).

646 L-Kynurenine, an amino acid identified as a sex pheromone in the urine of ovulated female

647 masu salmon. *Proc Natl Acad Sci USA* **103**(42), 15370-15374.

648 https://doi.org/10.1073/pnas.0604340103

649 Zeiske E, Theisen B & Breucker H (1992). Structure, development and evolutionary aspects of

650 the peripheral olfactory system. In *Fish Chemoreception*, Hara TJ (Ed.), pp. 13-39.

651 London: Chapman and Hall.

652

**Figure legends**

**Fig. 1.** Light microscopic organization of the olfactory organ of adult *Poecilia reticulata*. (**a**) In a frontal section of the head, the left olfactory organ appears composed of a single lamella (arrowheads) protruding into the olfactory cavity. (**b**) Histological organization of the olfactory epithelium (E) covering the olfactory lamella. LP, lamina propria. Hematoxylin-eosin. Scale bars (a), 200 μm; (b), 20 μm. ~~Gonads of 6-month-old *Poecilia reticulata* (Haematoxylin and Eosin). (**a**) Oocyte, characterized by abundant yolk and large lipid globules, in the adult ovary. (**b**) Spermatozoa located in groups of spermatozeugmata in the mature cysts of adult testis. Scale bar (1a, 1b), 100 μm.~~

**Fig. 2.** PCNA immunohistochemistry. (**a1, a2**) Representative micrographs of lamellae with mitotic cells in the basal layer (arrowheads) in 7-day-old female (a1) and male (a2) guppies. (**b1, b2**) Representative micrographs of lamellae in 45-day-old female (b1) and male (b2) guppies: dividing cells are more concentrated in the ~~caudal~~ posterior region of the olfactory organ (arrows) than in the basal layer of the central and rostral lamella (arrowhead). (**c1, c2**) Higher magnification of the caudal region of the olfactory lamella in 45-day-old female (c1) and male (c2). (**d1, d2**) Representative micrographs of the lamellae in adult female (d1) and male (d2) guppies: the PCNA-positive cells are mainly located in the ~~caudal~~ posterior edge of male olfactory organ (arrow), while in females they are also visible along the basal layer of the entire lamella (arrowheads). C, caudal; R, rostral; L, lateral; M, medial. Scale bars (a1-b2, d1, d2), 100 μm; (c1, c2), 10 μm. (**e**) Density of proliferating cells and statistical comparison among life stages and between sexes. (**f**) Volume of the olfactory lamella in adult females and males. Significant differences among stages are indicated by asterisks above the bars, while differences between sexes for each sampling time are indicated by asterisks superimposed on the bars.

677 Continuous lines, female/female comparison; dotted lines, male/male comparison. *$P<0.05$,

678 **$P<0.01$, N=10.

679

680 **Fig. 3.** $G_{\alpha\,olf}$ and calretinin immunohistochemistry. (**a**) Representative micrograph of lamellae

681 with $G_{\alpha\,olf}$-positive cells: immunostaining is mostly visible in the apical knobs of cOSNs

682 (arrows) but is also present in the cytoplasm of cells throughout the lower half of the epithelium

683 (arrowheads). Scale bar (a), 20 μm. (**b**) Optical density values of $G_{\alpha\,olf}$-positive cOSNs and

684 statistical comparison among life stages and between sexes. Asterisks indicate significant

685 male/female differences. *$P<0.05$, N=10. (**c**) Representative micrograph of lamellae with

686 calretinin-positive cells: they are mOSNs localized in the upper half of the epithelium. Scale

687 bar (c), 20 μm. (**d**) Optical density values of calretinin-positive mOSNs; there are no significant

688 differences among stages and between sexes.

689

690 **Fig. 4.** Calretinin-positive crypt cells. (**a, b**) Representative micrographs of stained crypt

691 neurons with the characteristic ovoid shape (arrows); in some cases, the emerging axon is

692 clearly visible (arrowhead). Scale bar (a, b): 20 μm. (**c**) Histogram comparing the number of

693 calretinin-positive crypt cells per animal at various life stages. (**d**) Histogram comparing the

694 density of calretinin-positive crypt cells at various life stages. Significant differences among

695 stages are indicated by asterisks above the bars, while differences between sexes for each

696 sampling time are indicated by asterisks superimposed on the bars. Continuous lines,

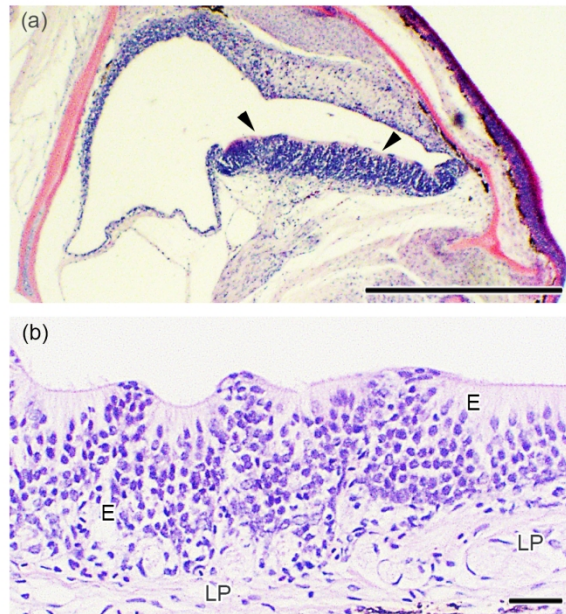697 female/female comparison; dotted lines, male/male comparison. *$P<0.05$, **$P<0.01$, N=10.

698

Fig. 1. Light microscopic organization of the olfactory organ of Poecilia reticulata
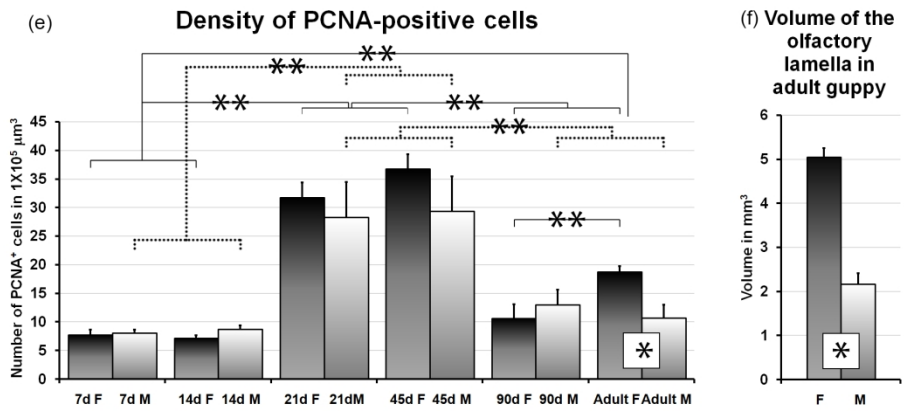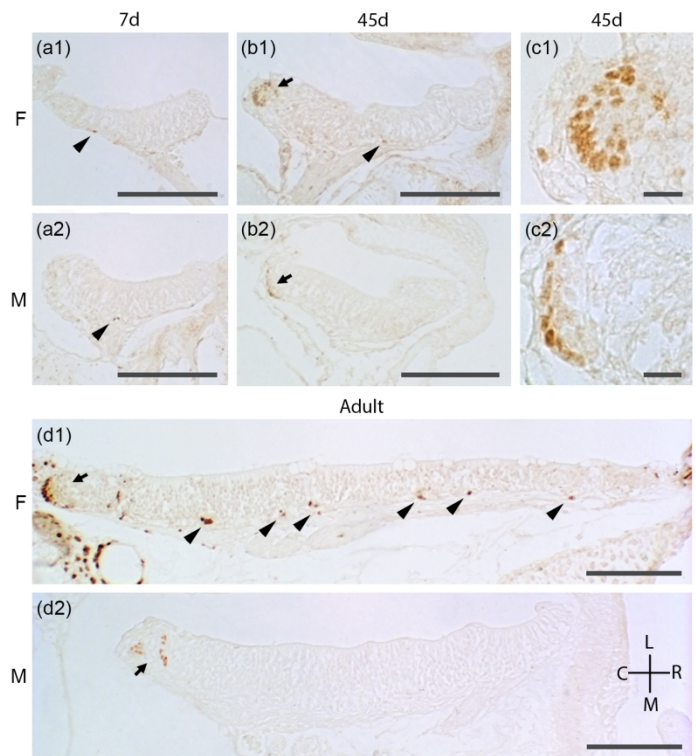
161x108mm (300 x 300 DPI)

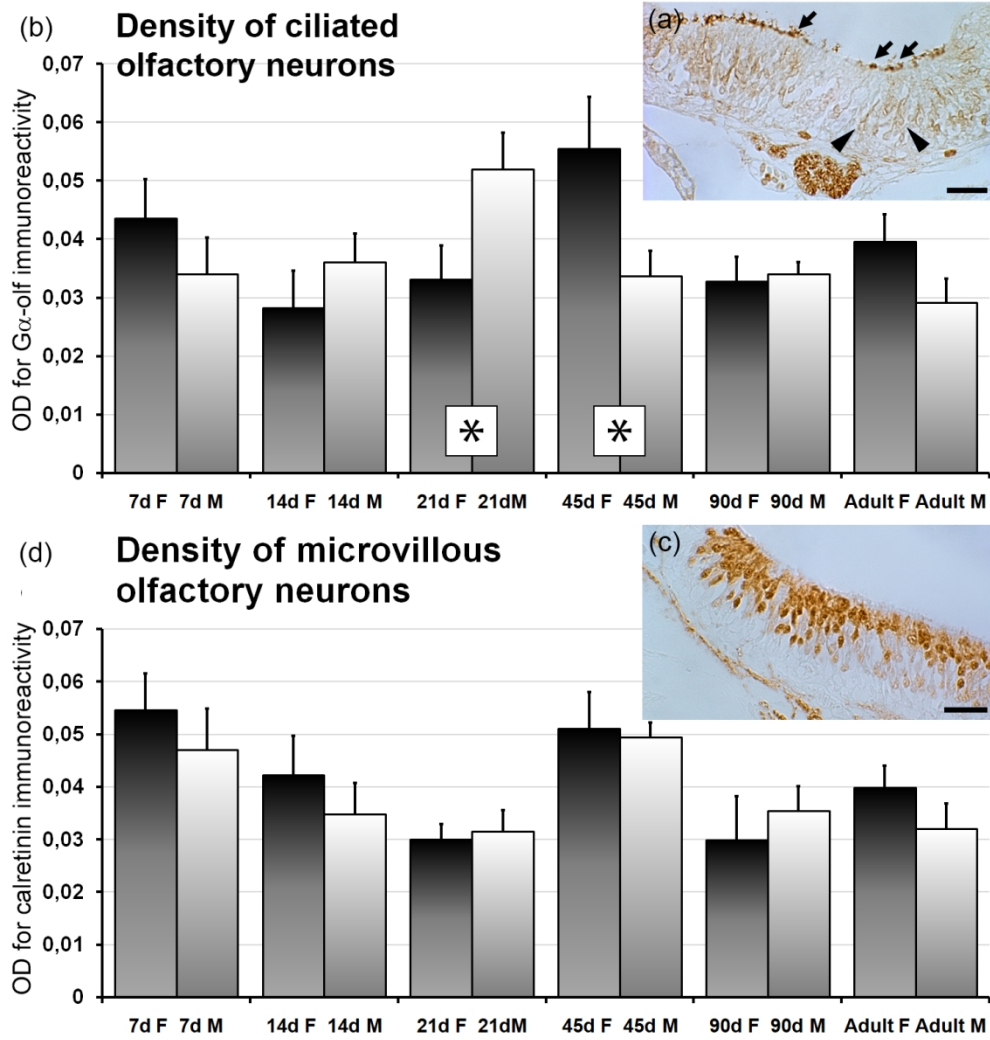Fig. 2. PCNA immunohistochemistry

162x216mm (300 x 300 DPI)

Fig. 3. $G_{\alpha\ olf}$ and calretinin immunohistochemistry.
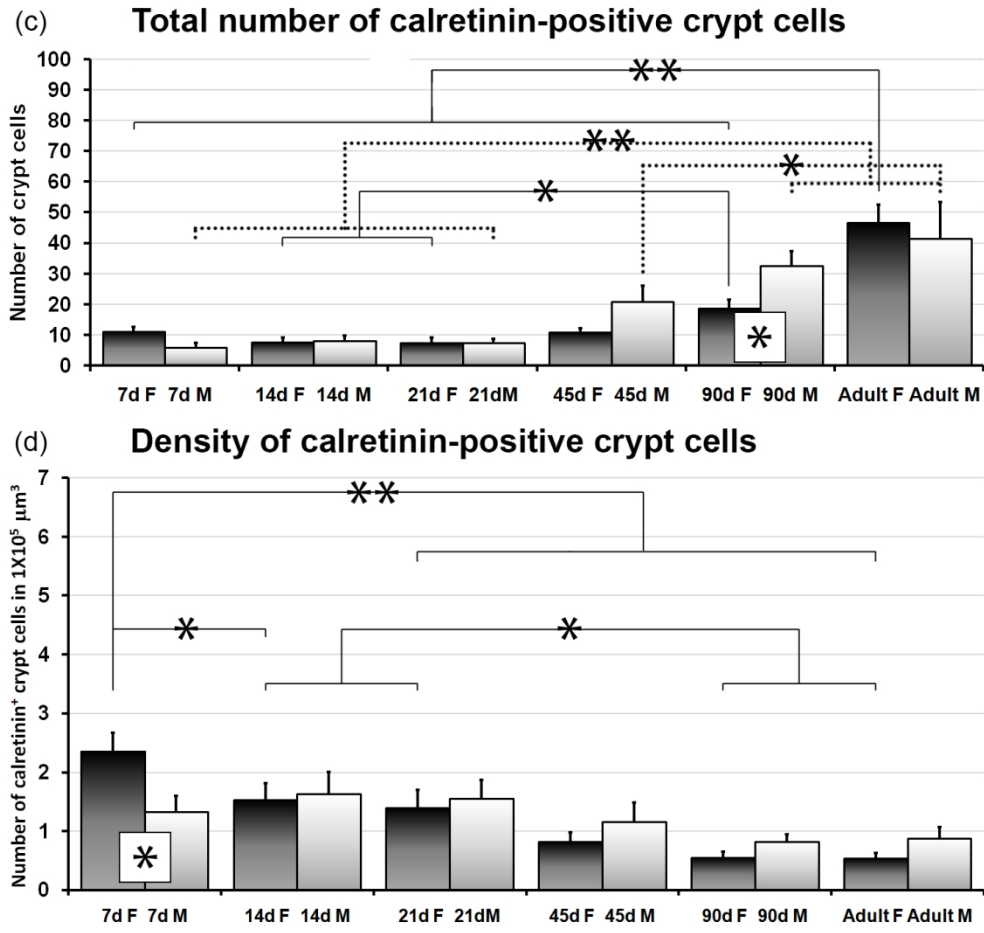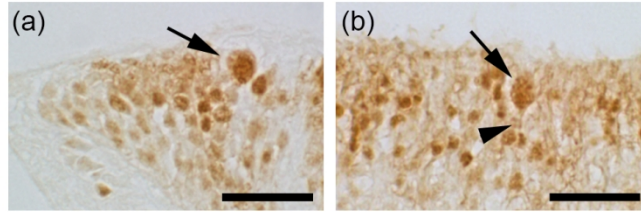
127x133mm (300 x 300 DPI)

Fig. 4. Calretinin-positive crypt cells.

127x151mm (300 x 300 DPI)

**Table 1.** Number of calretinin-positive crypt cells, total number of crypt cells (S100-positive)*, and their percentage ratio according to age and sex.

| FEMALE | Calretinin$^+$ crypt cells | Total number of crypt cells (S100$^+$) | $\dfrac{\text{Calretinin}^+ \text{ crypt cells}}{\text{S100}^+ \text{ crypt cells}}$ % |
|---|---|---|---|
| 7d | 10.8±1.3 | 13.8±1.4 | 77.93% |
| 14d | 7.7±1.3 | 9.2±1.7 | 84.28% |
| 21d | 7.4±1.8 | 8.4±1.3 | 88.02% |
| 45d | 10.9±1.3 | 27±3 | 40.62% |
| 90d | 19±3 | 77±6 | 24.36% |
| Adult | 47±6 | 297±30 | 15.74% |

| MALE | Calretinin$^+$ crypt cells | Total number of crypt cells (S100$^+$) | $\dfrac{\text{Calretinin}^+ \text{ crypt cells}}{\text{S100}^+ \text{ crypt cells}}$ % |
|---|---|---|---|
| 7d | 5.97±1.5 | 8.5±1.5 | 70.65% |
| 14d | 7.98±1.8 | 8.7±0.8 | 91.4% |
| 21d | 7.48±1.3 | 9.9±0.9 | 75.4% |
| 45d | 21±5 | 28±2 | 74.81% |
| 90d | 33±5 | 61±5 | 53.81% |
| Adult | 42±12 | 139±12 | 29.82% |

Values are mean per animal ± s.e.m.

* Values taken from Bettini et al., 2009, 2012